

Reference Interaction Site Model and Optimized Perturbation theories of colloidal dumbbells with increasing anisotropy

Gianmarco Munaò^{1,*,a)} Francisco Gámez^{2,1} Dino Costa^{1,1} Carlo Caccamo^{1,1} Francesco Sciortino^{3,1} and Achille Giacometti^{4,1}

¹*Dipartimento di Fisica e di Scienze della Terra, Università degli Studi di Messina, Viale F. Stagno d'Alcontres 31, 98166 Messina, Italy*

²*C/Clavel 101, Mairena del Aljarafe, 41927 Seville, Spain*

³*Dipartimento di Fisica and CNR-ISC, Università di Roma "Sapienza", Piazzale Aldo Moro 2, 00185 Roma, Italy*

⁴*Dipartimento di Scienze Molecolari e Nanosistemi, Università Ca' Foscari Venezia, Calle Larga S.Marta DD2137, Venezia I-30123, Italy*

We investigate thermodynamic properties of anisotropic colloidal dumbbells in the frameworks provided by the Reference Interaction Site Model (RISM) theory and an Optimized Perturbation Theory (OPT), this latter based on a fourth-order high-temperature perturbative expansion of the free energy, recently generalized to molecular fluids. Our model is constituted by two identical tangent hard spheres surrounded by square-well attractions with same widths and progressively different depths. Gas-liquid coexistence curves are obtained by predicting pressures, free energies, and chemical potentials. In comparison with previous simulation results, RISM and OPT agree in reproducing the progressive reduction of the gas-liquid phase separation as the anisotropy of the interaction potential becomes more pronounced; in particular, the RISM theory provides reasonable predictions for all coexistence curves, bar the strong anisotropy regime, whereas OPT performs generally less well. Both theories predict a linear dependence of the critical temperature on the interaction strength, reproducing in this way the mean-field behavior observed in simulations; the critical density – that drastically drops as the anisotropy increases – turns to be less accurate. Our results appear as a robust benchmark for further theoretical studies, in support to the simulation approach, of self-assembly in model colloidal systems.

I. INTRODUCTION

In recent years, a considerable number of experimental^{1–7} and numerical^{8–12} studies have been devoted to the investigation of phase behavior and self-assembly properties of colloidal dumbbells. Specific interest in this class stems essentially from the possibility to accurately tune the aspect ratio of the constituting spheres, as well as their interaction properties, so to obtain rich and fascinating phase behaviors.^{13–15} In particular, if one of the two particles is solvophilic and the other one is solvophobic, colloidal dumbbells represent a simple example of surfactant (Janus dumbbells),^{16,17} constituting a molecular generalization of Janus spherical particles,^{18–20} largely investigated in the last years because of their peculiar self-assembly properties and phase behaviors.^{21–27}

While a large number of experimental and numerical investigations have involved colloidal dumbbells, considerable less attention has been paid to theoretical studies: the framework of potential energy landscape has been adopted to describe the self-assembly of dumbbells into helices;²⁸ the competition between self-assembly and phase separation has been documented by integral equation theories;²⁹ the same approach^{30,31} and fundamental measure theory³² have been adopted to investigate structure and thermodynamics of hard dumbbells. Notwithstanding all such studies, a systematic theoretical de-

scription of the phase behavior of colloidal dumbbells is still lacking. In order to fill this gap, here we calculate systematically free energy, pressure, chemical potential and phase diagram of anisotropic colloidal dumbbells, so to investigate how such properties change by tuning the interaction potential. We consider to this task a series of model dumbbells constituted by two identical tangent hard spheres surrounded by square-well attractions with same widths and progressively different depths. We carry out our investigation in the frameworks provided by the Reference Interaction Site Model theory (RISM)³³ and a recently proposed Optimized Perturbation Theory (OPT).^{34,35} Theoretical predictions for the gas-liquid phase coexistence are compared with previous Monte Carlo results by us¹³ and other authors.³⁶ The present work extends our preliminary OPT analysis of the symmetric case³⁵ and our RISM study on a slightly different dumbbell model.²⁹

As for the RISM theory,³³ it constitutes a molecular generalization of the Ornstein-Zernike theory of simple fluids.³⁷ Originally devised for rigid molecules constituted by hard spheres,³⁸ the theory was later extended to more complex systems, like colloidal models; in particular, it was used to investigate the thermodynamic and structural properties of discotic lamellar colloids,^{39,40} the self-assembly in diblock copolymers modeled as “ultra-soft” colloids,⁴¹ the interaction between colloidal particles and macromolecules,⁴² the crystallization and solvation properties of nanoparticles in aqueous solutions,⁴³ the liquid structure of tetrahedral colloidal particles⁴⁴, and the self-assembly properties of Janus rods.⁴⁵

^{a)}Corresponding author, email: gmunao@unime.it

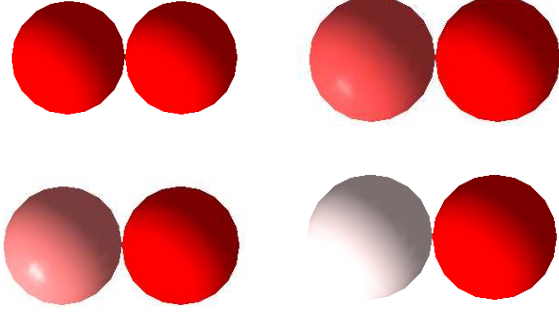


FIG. 1. Schematic representation of colloidal dumbbells investigated in this work. Starting from the symmetric case $\varepsilon_{11} = \varepsilon_{12} = \varepsilon_{22}$ (top, left), the interaction becomes progressively asymmetric by reducing $\varepsilon_{11} = \varepsilon_{12} = 0.7, 0.5, 0.3, 0.1\varepsilon_{22}$. The weakening of ε_{11} is signaled by progressively “fading” the color of the first site.

As for the perturbation theory, this scheme played a significant role in describing the thermodynamic properties of a large variety of fluids.^{46–51} The theory was originally proposed as a high-temperature expansion by several groups and then recast in a very efficient computational tool by Barker and Henderson.^{52–54} It has been recently adapted to cope with Janus⁵⁵ and tri-block Janus⁵⁶ fluids. Here we use an optimized version of this theory based on a fourth-order high-temperature perturbative expansion of the free energy, recently developed to fit a large set of simulation data for square-well fluids.³⁴ Recently, one of the authors generalized this approach to deal with more complex systems, like molecular fluids.³⁵ Within this formalism, the effective energy and range of square-well interactions depend on the molecular anisotropy. In this way, it is possible to calculate analytical equations of state for a large variety of molecular models like for instance dimers, trimers, chains and spherocylinders.³⁵

The importance of assessing the accuracy of these theoretical approaches is crucial, as a large number of demanding numerical calculations¹⁴ is typically required to investigate the experimentally relevant heterogeneous dumbbells case.³ A reliable theoretical tool would then help to focus on those systems of great interest.

The paper is organized as follows: in Section II we provide the details of interaction potential and RISM and OPT schemes. Results are presented and discussed in Section III and conclusions follow in Section IV.

II. MODELS AND THEORIES

A. Interaction potentials

The sequence of models investigated in this work is schematically represented in Fig. 1: they are constituted

by two identical tangent hard spheres of diameter σ , labeled as 1 and 2, interacting with sites 1 and 2 of another dumbbell at distance r via square-well (SW) attractions with same width ($\lambda = 0.5$) and different depths ε_{ij} ($i, j = 1, 2$):

$$V_{ij}(r) = \begin{cases} \infty & \text{if } r < \sigma \\ -\varepsilon_{ij} & \text{if } \sigma \leq r < \sigma + \lambda\sigma \\ 0 & \text{otherwise.} \end{cases} \quad (1)$$

Parameters σ and ε_{22} provide, respectively, the unit of length and energy, in which terms we define the reduced temperature $T^* = k_B T / \varepsilon_{22}$ (with k_B as the Boltzmann constant), number density $\rho^* = \rho \sigma^3$ and pressure $P^* = P \sigma^3 / \varepsilon_{22}$. In all calculations we have fixed $\varepsilon_{12} (\equiv \varepsilon_{21}) = \varepsilon_{11}$; then, we have studied a sequence of cases obtained by progressively reducing ε_{11} starting from the symmetric case, $\varepsilon_{11} = \varepsilon_{22}$, to $\varepsilon_{11} = 0.7, 0.3, 0.1$ (in units of ε_{22}).

B. Reference interaction site model theory

In the RISM framework³³ the pair structure of a fluid composed by identical two-site molecules is characterized by a set of four site-site intermolecular pair correlation functions $h_{ij}(r) = g_{ij}(r) - 1$ where $(i, j) = (1, 2)$ and $g_{ij}(r)$ are the site-site radial distribution functions. The $h_{ij}(r)$ are related to a set of intermolecular direct correlation functions $c_{ij}(r)$ by a matrix generalization of the Ornstein-Zernike equation for simple fluids,³⁷ expressed in the k -space as:

$$\mathbf{H}(k) = \mathbf{W}(k)\mathbf{C}(k)\mathbf{W}(k) + \rho\mathbf{W}(k)\mathbf{C}(k)\mathbf{H}(k), \quad (2)$$

where $\mathbf{H} \equiv [h_{ij}(k)]$, $\mathbf{C} \equiv [c_{ij}(k)]$, and $\mathbf{W} \equiv [w_{ij}(k)]$ are 2×2 symmetric matrices; the elements $w_{ij}(k)$ are the Fourier transforms of the intramolecular correlation functions, written explicitly as:

$$w_{ij}(k) = \frac{\sin[kL_{ij}]}{kL_{ij}}, \quad (3)$$

where the bond length L_{ij} is given either by $L_{ij} = \sigma$, if $i \neq j$, or by $L_{ij} = 0$, otherwise. In order to solve the RISM equation (2), we have adopted in this work the Kovalenko-Hirata (KH) closure^{57,58} that assumes — beside the exact expression $g_{ij}(r) = 0$ if $r \leq \sigma$ — the direct correlation functions outside the hard-core to be approximated by a combination of the Mean Spherical Approximation (MSA) and HyperNetted Chain (HNC) expression:³⁷

$$\begin{aligned} c_{ij}(r) &= \begin{cases} \text{HNC} & \text{if } g_{ij}(r) \leq 1 \\ \text{MSA} & \text{if } g_{ij}(r) > 1 \end{cases} \\ &\equiv \begin{cases} \exp[-\beta V_{ij}(r) + \gamma_{ij}(r)] - \gamma_{ij}(r) - 1 \\ -\beta V_{ij}(r), \end{cases} \end{aligned} \quad (4)$$

where $\beta = 1/T^*$ and $\gamma_{ij}(r) = h_{ij}(r) - c_{ij}(r)$. We have implemented the numerical solution of the RISM/KH

scheme by means of a standard iterative Picard algorithm, on a grid of 8192 points with a mesh $\Delta r = 0.005\sigma$.

In order to calculate the thermodynamic properties, we have used standard thermodynamic integration formulæ³⁷ that already proven to be successful for SW dumbbells.²⁹ Specifically, we have calculated the excess free energy per particle via the energy route along constant-density paths according to:

$$\frac{\beta F^{\text{ex}}(\beta)}{N} = \frac{\beta F^{\text{ex}}(\beta = 0)}{N} + \int_0^\beta \frac{U(\beta')}{N} d\beta', \quad (5)$$

where $U(\beta)$ is the internal energy of the fluid at a given inverse temperature β and $F^{\text{ex}}(\beta = 0)$ corresponds to the excess free energy of tangent hard-sphere dumbbells. For this, the most classical expressions known in the literature are an analytic expression due to Tildesley and Street⁵⁹ (and devised to fit their Monte Carlo data) and the Wertheim equation of state for tangent hard dumbbells,⁶⁰ reading:

$$\begin{aligned} \frac{\beta F^{\text{ex}}(\beta = 0)}{N} = & n \frac{(4\eta - 3\eta^2)}{(1 - \eta)^2} \\ & + (n - 1) \left[3 \ln(1 - \eta) + \ln \left(\frac{2}{2 - \eta} \right) \right] \\ & + \ln(6\eta/\pi) - 1, \end{aligned} \quad (6)$$

where $\eta = 2(\pi/6)\rho^*$ is the dumbbell packing fraction. We have explicitly verified that such equation agrees with the free energy expression for hard dumbbells provided in Ref. 59. Equation (6) has the additional advantage to avoid free parameters and the fit of simulation data, so that we will use it through all the calculations.

The excess pressure is then obtained through the (numerical) derivative of the l.h.s. of Eq. (5) with respect to the density, taken at constant temperature, while coexistence conditions are determined by searching for equal chemical potentials and pressures (at a given temperature) of the two coexisting phases. Finally, critical temperatures and densities are obtained by fitting the coexistence points through the scaling law for the densities and the law of rectilinear diameters with an effective critical exponent $\delta=0.32$.⁶¹ We refer the reader to our previous work²⁹ for full details on the above procedure.

Using the symmetric model as a test case, we have also investigated the quality of predictions obtained by different approaches within the RISM framework. Specifically, we have studied the HNC closure, that assumes expressions in the top lines of Eq. (4) holding for all $r > \sigma$ independently on the value of $g(r)$. Moreover, within the KH closure, we have studied a different route from structure to thermodynamics, based on closed formulæ (i.e requiring no thermodynamic integration) to calculate free energy and pressure. Such expressions, derived by Kovalenko and Hirata in Refs. 57 and 58, closely follow the corresponding relations deduced long ago⁶² within the Ornstein-Zernike/HNC scheme for simple fluids and later generalized to the RISM/HNC scheme.⁶³ We refer

the reader to the original works and our recent application⁴⁴ for full details.

C. Optimized perturbation theory

The starting point of OPT is given by the optimized equation of state recently proposed in Ref. 34, where the free energy of a fluid composed by SW particles with well depth ε and width λ , at temperature T and density ρ is expressed as a perturbation series in the form:

$$\frac{\beta F(\beta)}{N} = \frac{\beta F(\beta = 0)}{N} + \sum_{m=1}^{\infty} \left[\frac{\varepsilon}{k_B T} \right]^m f_m(\rho, \lambda). \quad (7)$$

In Eq. (7) $F^{\text{ex}}(\beta = 0)$ is the free energy of the reference hard-sphere fluid plus the ideal contribution, and f_m are m -th order perturbation terms. In Ref. 34 the series is truncated, and f_m are calculated up to the fourth-order. The theory includes the Barker-Henderson⁵² result as a truncation of the expansion to second order. The third and fourth orders, however, are not included as explicit higher order corrections to the Barker-Henderson theory, that would require uncontrolled truncations of the hierarchy of correlation functions, but as an optimized phenomenological calculation of coefficients, hinging on simulations results.³⁴ It turns out that this theory for the SW fluid is accurate over nearly the whole density range and subcritical (low) temperatures. We refer the reader to the original work³⁴ for detailed expressions of f_m ($m = 1, \dots, 4$), as well as all other necessary machinery.

The OPT generalization at issue, pertinent to a fluid composed by SW dumbbells, is written explicitly as a sum of SW contributions, each taking separately into account the four $(i, j = 1, 2)$ interactions of Eq. (1), in the form:³⁵

$$\frac{\beta F(\beta)}{N} = \frac{\beta F(0)}{N} + \sum_{i,j=1}^2 \left\{ \sum_{m=1}^4 \left[\frac{\varepsilon_{ij}}{k_B T} \right]^m f_m(\rho, \lambda) \right\}. \quad (8)$$

As visible, each term in the free energy expansion is weighted by a temperature reduced by the corresponding well depth ε_{ij} , ρ is the density of sites 1 or 2, and λ takes the fixed value 0.5. Given the spherical symmetry of each site-site interaction, the molecular anisotropy is taken into account by the reference free energy, provided in our case by the Wertheim equation of state for tangent hard dumbbells of Eq. (6).⁶⁰ This choice gives better results for non-convex particles in comparison with the possibility to define an effective hard-sphere diameter with the corresponding scaling of density.³⁵; it turns out to be accurate for a moderate number of beads per chain.

Given Eq. (8), one can obtain the thermodynamic properties from usual thermodynamic relations. For instance, the compressibility factor

$$Z \equiv \frac{\beta P}{\rho} = 1 + \eta \frac{\partial}{\partial \eta} \left[\frac{\beta F^{\text{ex}}}{N} \right]_T \quad (9)$$

can also be expressed as a high-temperature expansion,

$$Z = 1 + Z^{\text{ex}}(\beta = 0) + \sum_{i,j=1}^2 \left\{ \sum_{m=1}^{\infty} \left[\frac{\varepsilon_{ij}}{k_B T} \right]^m z_m(\rho, \lambda) \right\}, \quad (10)$$

where $z_m = \eta \partial / \partial \eta [f_m(\rho, \lambda)]_T$.

As in the RISM framework, we have determined the gas-liquid phase boundaries by the condition of thermal, mechanical, and chemical equilibrium. Numerical methods have been used to this task, based in this case on a combination of the Levenberg-Marquardt algorithm with Gauss and steepest-descent methods.⁶⁵

III. RESULTS

In Fig. 2 we compare the energy-route KH and OPT predictions for symmetric colloidal dumbbells, i.e. with $\varepsilon_{11} = \varepsilon_{22}$ in Eq. (1). Results for the pressure (a) and free energy (b) are reported along different isotherms across the critical temperature $T_c^* \approx 1.60$ (estimated in our previous work).¹³ KH and OPT predict the same trends both for the pressure and free energy; in particular, they provide evidence for a supercritical fluid at $T^* = 1.90$, whereas a van der Waals loop — heralding a gas-liquid phase separation — develops at $T^* = 1.60$ and becomes well defined at $T^* = 1.40$. The quantitative agreement between the two theories slightly worsens at low temperatures, where OPT curves fall progressively below the corresponding KH ones; this circumstance implies a higher OPT critical temperature and, correspondingly, a wider gas-liquid coexistence curve. In Fig. 2c we compare KH gas-liquid coexistence curves — as obtained by the energy route and the closed formulæ — with Monte Carlo (MC) data by us¹³ and other authors.³⁶ OPT predictions, already provided in Ref. 35, are also reported for comparison. One can notice that KH reproduces reasonably well all features, whereas OPT, as observed, overestimates the two-phase region. Such a discrepancy could be possibly ascribed to the truncation involved in the OPT procedure (see Eq. (8)). In this case improvements could be achieved by incorporating higher order terms in the free energy expansion, so to take into account more accurately density fluctuations, along the lines described for instance in Ref. 64. In general, the OPT scheme for SW dumbbells shares the same level of accuracy of the original approach for the SW atomic fluid,³⁴ the latter performing slightly better in the critical region.

As for HNC, we have verified that at high temperatures no significant differences arise with the pressure calculated within the KH scheme (see the curves corresponding to $T^* = 1.90$ in the inset of Fig. 2a). On the other hand, upon lowering the temperature, the numerical convergence of HNC becomes progressively more problematic, thus precluding from further exploration a progressively larger interval of $T-\rho$ conditions. As a consequence, the conditions for gas-liquid coexistence turn to be completely unattainable. This issue is even more

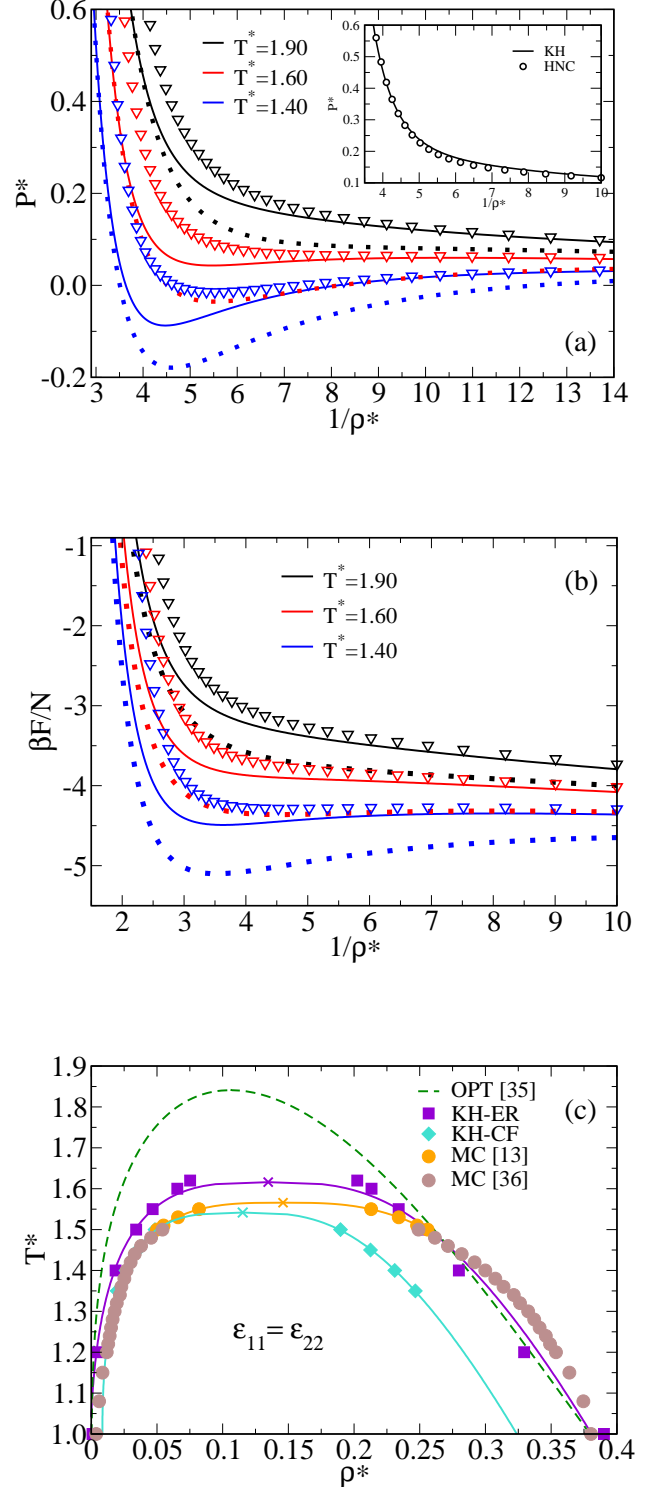


FIG. 2. Pressure (a) and free energy (b) of symmetric colloidal dumbbells along different isotherms (see legends): KH energy route (lines), KH closed formulæ (triangles) and OPT (small squares). In the inset, KH and HNC energy-route pressures at $T^* = 1.90$. Panel c: gas-liquid coexistence by KH energy-route (KH-ER, squares), KH closed formulæ (KH-CF, diamonds), OPT (dashed line)³⁵ and MC (circles).^{13,36} Full lines are best-fits of KH and simulation points (see text) with corresponding critical points (crosses).

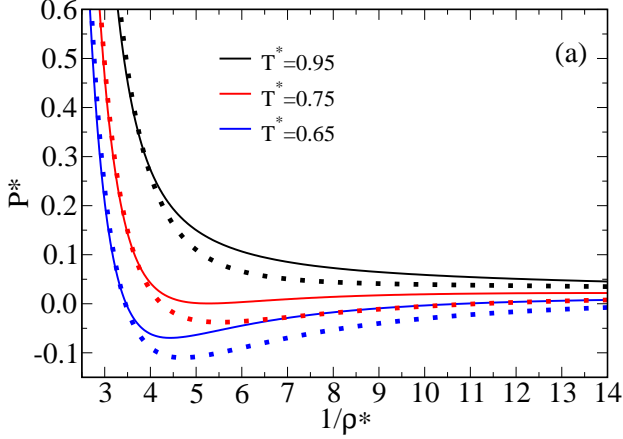


FIG. 3. KH (lines) and OPT (small squares) pressures of colloidal dumbbells with $\varepsilon_{11} = 0.3\varepsilon_{22}$.

pronounced as the molecular anisotropy increases, leaving KH and OPT schemes as the only reliable approaches to study the phase separation properties of our models.

As for KH closed formulæ, pressures and free energies at different temperatures are also reported in Fig. 2. As visible, a van der Waals loop in the pressure is observed in the same range of temperatures of KH energy route and OPT, even if systematically higher and shallower estimates are obtained. The same discrepancy appears to affect the predictions for the free energy. As a result (see Fig. 2c), the liquid branch of phase coexistence appears too low in comparison with simulations, KH energy route and OPT, whereas the critical temperature and the whole gas branch turn to be quite well predicted. Overall, the KH energy route appears more accurate and therefore we shall adopt such a scheme — together with the differently based OPT approach — to investigate the phase behavior of other cases with $\varepsilon_{11} < \varepsilon_{22}$.

As visible from Fig. 3, the agreement between KH and OPT predictions for the pressure essentially persists as ε_{11} is reduced down to $0.3\varepsilon_{22}$. In Ref. 13 we have documented the progressive shrinkage of the coexistence curves toward low temperatures as ε_{11} is reduced. As visible from Fig. 4, where coexistence curves for $\varepsilon_{11} = 0.7$, 0.5 , and $0.3\varepsilon_{22}$ are reported, this feature is reproduced by both theories, essentially at the same level of accuracy observed for the symmetric case: KH still provides reasonable estimates of the gas-liquid coexistence curve, with critical temperatures and densities fairly well predicted, whereas OPT overestimates the amplitude of the two-phase region and, accordingly, the critical temperature.

As documented in our recent simulation study,¹³ increasing the asymmetry of total interaction promotes the development of aggregates in the fluid; specifically

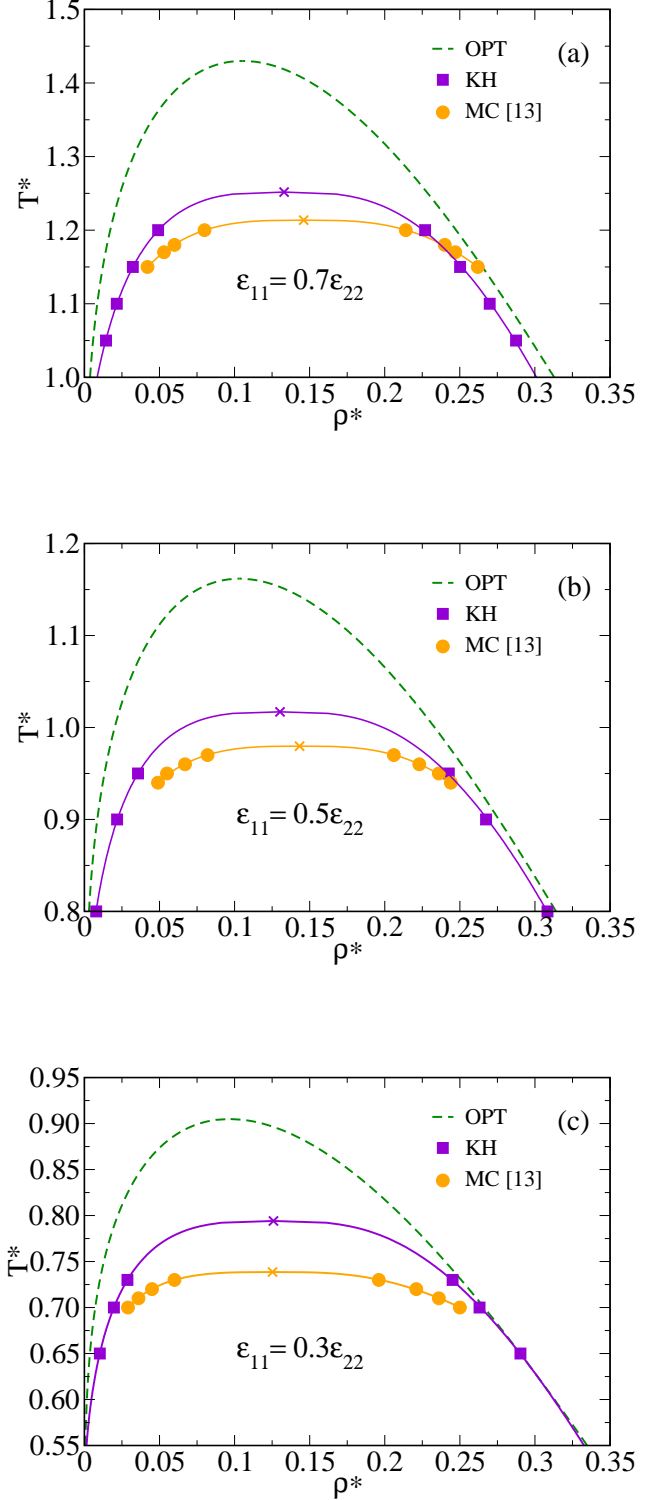


FIG. 4. Gas-liquid coexistence curves of colloidal dumbbells upon progressively decreasing ε_{11} .

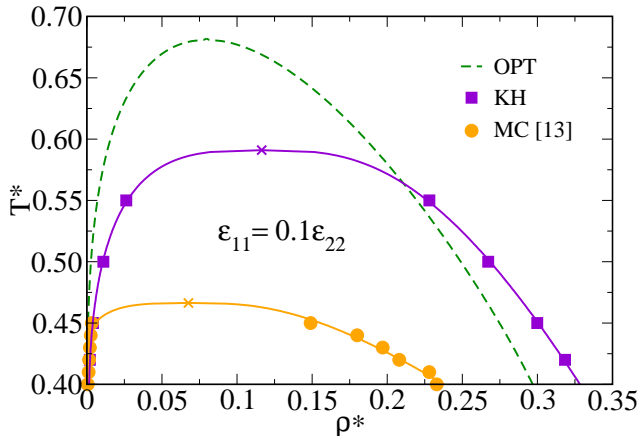


FIG. 5. Gas-liquid coexistence of colloidal dumbbells with $\varepsilon_{11} = 0.1\varepsilon_{22}$.

at $\varepsilon_{11} = 0.1\varepsilon_{22}$, dumbbells self-assemble into micelles at low densities and planar structures (lamellæ) at intermediate/high densities, provided the temperature is low enough. Moreover the self-assembly process tends to destabilize the gas-liquid phase separation – completely disappearing for Janus dumbbells, i.e. with $\varepsilon_{11} = 0$ — with the coexistence curve stretched toward very low gas densities and a critical temperature drastically lower than in the symmetric case. At variance with previous cases, both KH and OPT theories fail to reproduce such a behavior, largely overestimating the coexistence region at $\varepsilon_{11} = 0.1\varepsilon_{22}$, as visible in Fig. 5.

Indeed, we may surmise that liquid state theories, explicitly tailored to describe a homogeneous fluid environment, progressively worsen as local inhomogeneities tend to develop in the system. Also, the progressive displacement of binodal curves toward lower temperatures may negatively affect the OPT predictions based, as described, on a high-temperature expansion of the free energy.

Numerical values of KH, OPT and MC critical parameters for all ε_{11} investigated in this work are collectively reported in Tab. I. Critical temperatures and densities as functions of ε_{11} are shown in Fig. 6. Remarkably, both theories agree with simulations in providing a linear dependence of the critical temperature on ε_{11} . Such a circumstance is compatible with a mean field behavior,¹³ with the only exception (for MC data) of the $\varepsilon_{11} = 0.1\varepsilon_{22}$ case. Conversely, the critical density ρ_c^* follows quite a different trend, keeping an almost constant value from the symmetric case down to $\varepsilon_{11} = 0.5\varepsilon_{22}$, with a marked drop upon further lowering this parameter. Surprisingly enough, OPT qualitatively reproduces such a behavior, actually predicting a critical density close to simulation data for $\varepsilon_{11} = 0.1\varepsilon_{22}$. On the other hand, the dependence

TABLE I. Critical temperatures, densities and chemical potentials for colloidal dumbbells with variable ε_{11} as obtained by MC,¹³ KH and OPT.

$\varepsilon_{11}/\varepsilon_{22}$		T_c^*	ρ_c^*	μ_c/ε_{22}
1.0	MC	1.566	0.146	-5.680
	KH	1.616	0.135	-5.973
	OPT	1.842	0.106	-6.549
0.7	MC	1.213	0.146	-4.524
	KH	1.252	0.133	-4.610
	OPT	1.430	0.105	-5.025
0.5	MC	0.980	0.143	-3.725
	KH	1.017	0.130	-3.762
	OPT	1.162	0.103	-4.107
0.3	MC	0.739	0.125	-2.997
	KH	0.794	0.126	-2.964
	OPT	0.905	0.097	-3.248
0.1	MC	0.466	0.068	-2.635
	KH	0.591	0.116	-2.284
	OPT	0.682	0.080	-2.205

of KH ρ_c^* on ε_{11} is less pronounced, failing to reproduce in particular the very low values attained at $\varepsilon_{11} = 0.1\varepsilon_{22}$.

In a recent study,²⁹ we have analyzed the RISM performances for a close class of SW dumbbells, characterized for instance by an attraction range $\lambda = 0.1$, shorter than that investigated here (namely $\lambda = 0.5$). In that case we have shown that the HNC theory is able to describe the low temperature regime whereupon the gas-liquid coexistence takes place; in particular, the theory predicts the disappearance of a stable phase separation for $\varepsilon_{11} < 0.4\varepsilon_{22}$, i.e. at a value slightly larger than that observed in simulations ($\varepsilon_{11} < 0.2\varepsilon_{22}$). Also for $\lambda = 0.1$ RISM agrees with simulations in predicting the linear scaling of the critical temperature discussed in Fig. 6a, even if with a larger discrepancy with respect to the present case; a better agreement is instead observed for the critical density, essentially because this quantity, at $\lambda = 0.1$, keeps an almost constant value as a function of ε_{11} , at variance with the sudden drop documented in Fig. 6b.

IV. CONCLUSIONS

We have presented a theoretical study of thermodynamic properties and gas-liquid phase coexistence of anisotropic colloidal dumbbells, where the anisotropy stems from the fact that, although the two colloids forming the dumbbell are identical in sizes, their interactions are not, as one of the two attractive square-well depth is gradually reduced to zero toward the Janus dumbbells limit. We have discussed and contrasted to each other

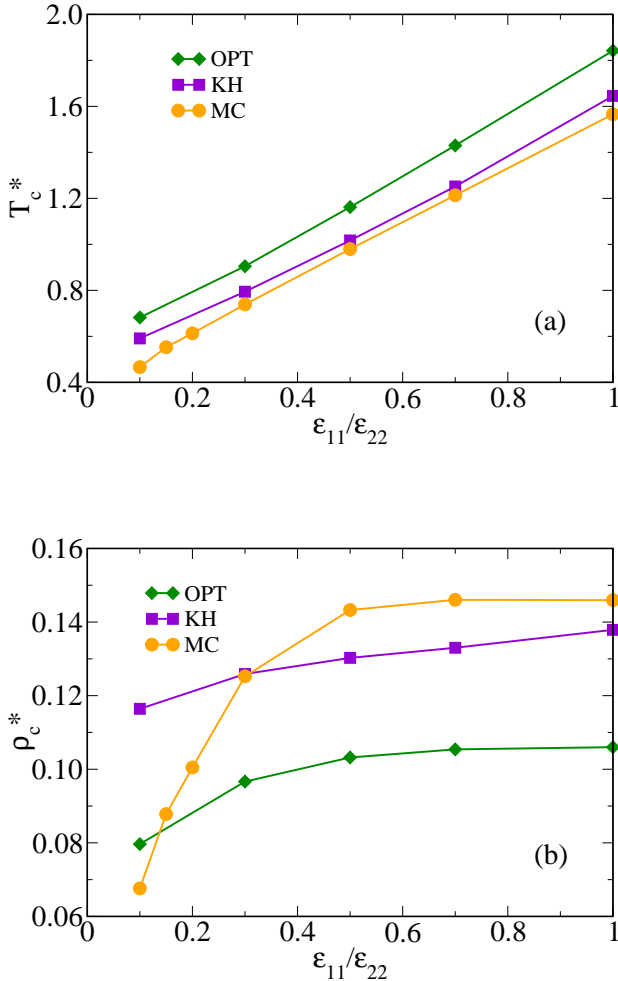


FIG. 6. Critical temperatures (a) and densities (b) of colloidal dumbbells as functions of ε_{11} .

the performances of two venerable and well established tools, the RISM and OPT theories of liquids. As for the RISM, this theory hinges on the solution of the integral equations of liquids, thus providing the intermolecular correlations, whereby all thermodynamic properties can be obtained. Using the symmetric model as a test case, we have shown that the Kovalenko-Hirata closure (combining efficiently MSA and HNC approximations) complemented with the energy route from structure to thermodynamics is superior to the HNC approximation and other procedures to calculate the thermodynamic properties. As for the OPT theory, this method hinges on a fourth-order high-temperature perturbative expansion of the free energy of the square-well fluid, recently generalized to deal with molecular fluids.

The accuracy of both methods has been assessed by a direct comparison with recent numerical simulations. We have found that both approaches provide reasonable

predictions, with RISM slightly outperforming OPT in almost all cases with the notable exception of the critical density, where OPT is more accurate. Latter predictions could be improved by finding a way to fully include in the formalism the intramolecular correlations, presently taken into account only at the level of the reference free energy.

We emphasize the importance of having a reliable theoretical tool to provide a quick estimate of thermodynamics of colloidal dumbbells. Recent experiments,⁶⁶ as well as complementary numerical work,¹⁴ show that in most of the interesting cases the two colloids forming the dumbbells are asymmetric both in size and interaction. This means that a huge number of possible combinations could be in principle studied to probe many topologically different resulting phase diagrams. A reliable theoretical approach would then be invaluable in pinning down the most interesting cases where a more sophisticated, and computationally more demanding, calculation could be performed.

ACKNOWLEDGMENTS

GM, DC, CC, FS, and AG gratefully acknowledge support from PRIN-MIUR 2010-2011 Project.

- ¹T. S. Skelton, Y. Chen, and S. A. F. Bon, *Soft Matter* **10**, 7730 (2014)
- ²F. Ma, S. Wang, H. Zao, D. T. Wu, and N. Wu, *Soft Matter* **10**, 8349 (2014)
- ³D. J. Kraft, R. Ni, F. Smalenburg, M. Hermes, K. Yoon, D. A. Weitz, A. van Blaaderen, J. Groenewold, M. Dijkstra, and W. Kegel, *Proceedings of the National Academy of Science (USA)* **109**, 10787 (2012)
- ⁴D. Nagao, K. Goto, H. Ishii, and M. Konno, *Langmuir* **27**, 13302 (2011)
- ⁵K. Yoon, D. Lee, J. W. Kim, J. Kim, and D. A. Weitz, *Chem. Comm.* **48**, 9056 (2012)
- ⁶J. D. Forster, J. G. Park, M. Mittal, H. Noh, C. F. Schreck, C. S. O'Hern, H. Cao, E. M. Furst, and E. R. Dufresne, *ACS Nano* **5**, 6695 (2011)
- ⁷I. D. Hosein and C. M. Liddell, *Langmuir* **23**, 10479 (2007)
- ⁸G. A. Chapela, F. del Río, and J. Alejandre, *J. Chem. Phys.* **134**, 224105 (2011)
- ⁹G. A. Chapela and J. Alejandre, *J. Chem. Phys.* **135**, 084126 (2011)
- ¹⁰M. A. Miller, R. Blaak, C. N. Lumb, and J.-P. Hansen, *J. Chem. Phys.* **130**, 114507 (2009)
- ¹¹P. Ilg and E. Del Gado, *Soft Matter* **7**, 163 (2011)
- ¹²S. H. Chong, A. J. Moreno, F. Sciortino, and W. Kob, *Phys. Rev. Lett.* **94**, 215701 (2005)
- ¹³G. Munaò, P. O'Toole, T. S. Hudson, D. Costa, C. Caccamo, A. Giacometti, and F. Sciortino, *Soft Matter* **10**, 5269 (2014)
- ¹⁴G. Munaò, P. O'Toole, T. S. Hudson, D. Costa, C. Caccamo, F. Sciortino, and A. Giacometti, *J. Phys. Condens. Matter*, in press (2015)
- ¹⁵G. Avvisati, T. Vissers, and M. Dijkstra, *J. Chem. Phys.* **142**, 084905 (2015)
- ¹⁶F. Tu, B. J. Park, and D. Lee, *Langmuir* **29**, 12679 (2013)
- ¹⁷B. J. Park and D. Lee, *ACS Nano* **6**, 782 (2012)
- ¹⁸L. Hong, A. Cacciuto, E. Luijten, and S. Granick, *Langmuir* **24**, 621 (2008)
- ¹⁹C.-H. Chen, R. K. Shah, A. R. Abate, and D. A. Weitz, *Langmuir* **25**, 4320 (2009)

- ²⁰B. S. Jiang, Q. Chen, M. Tripathy, E. Luijten, K. S. Schweizer, and S. Granick, *Advanced Materials* **22**, 1060 (2010)
- ²¹L. Hong, A. Cacciuto, E. Luijten, and S. Granick, *Nano Letters* **6**, 2510 (2006)
- ²²Q. Chen, J. K. Whitmer, S. Jiang, S. C. Bae, E. Luijten, and S. Granick, *Science* **331**, 199 (2011)
- ²³Q. Chen, J. Yan, J. Zhang, S. C. Bae, and S. Granick, *Langmuir* **28**, 1355 (2012)
- ²⁴J. Yan, M. Bloom, S. C. Bae, E. Luijten, and S. Granick, *Nature* **491**, 578 (2012)
- ²⁵F. Sciortino, A. Giacometti, and G. Pastore, *Phys. Rev. Lett.* **103**, 237801 (Dec. 2009)
- ²⁶F. Sciortino, A. Giacometti, and G. Pastore, *Phys. Chem. Chem. Phys.* **12**, 11869 (2010)
- ²⁷T. Vissers, Z. Preisler, F. Smallenburg, M. Dijkstra, and F. Sciortino, *J. Chem. Phys.* **138**, 164505 (2013)
- ²⁸S. N. Fejer, D. Chakrabarti, H. Kusumaatmaja, and D. J. Wales, *Nanoscale* **6**, 9448 (2014)
- ²⁹G. Munaò, D. Costa, A. Giacometti, C. Caccamo, and F. Sciortino, *Phys. Chem. Chem. Phys.* **15**, 20590 (2013)
- ³⁰G. Munaò, D. Costa, and C. Caccamo, *Chem. Phys. Lett.* **470**, 240 (2009)
- ³¹G. Munaò, D. Costa, and C. Caccamo, *J. Chem. Phys.* **130**, 144504 (2009)
- ³²M. Marechal, H. H. Goetzke, A. Härtel, and H. Löwen, *J. Chem. Phys.* **135**, 234510 (2011)
- ³³D. Chandler and H. C. Andersen, *J. Chem. Phys.* **57**, 1930 (1972)
- ³⁴R. Espíndola-Heredia, F. del Río, and A. Malijevský, *J. Chem. Phys.* **130**, 024509 (2009)
- ³⁵F. Gámez, *J. Chem. Phys.* **140**, 234504 (2014)
- ³⁶L. Li, K. Tang, L. Wu, W. Zhao, and J. Cai, *J. Chem. Phys.* **136**, 214508 (2012)
- ³⁷J.-P. Hansen and I. R. McDonald, *Theory of simple liquids*, 3rd Ed. (Academic Press, New York, 2006)
- ³⁸L. J. Lowden and D. Chandler, *J. Chem. Phys.* **61**, 5228 (1974)
- ³⁹L. Harnau, J.-P. Hansen, and D. Costa, *Europhys. Lett.* **53**, 729 (2001)
- ⁴⁰D. Costa, J.-P. Hansen, and L. Harnau, *Mol. Phys.* **103**, 1917 (2005)
- ⁴¹J.-P. Hansen and C. Pearson, *Mol. Phys.* **104**, 3389 (2006)
- ⁴²P. G. Khalatur, L. V. Zherenkova, and A. R. Khokhlov, *J. Phys. II (France)* **7**, 543 (1997)
- ⁴³W. Kung, P. González-Mozuelos, and M. O. de la Cruz, *Soft Matter* **6**, 331 (2010)
- ⁴⁴G. Munaò, D. Costa, F. Sciortino, and C. Caccamo, *J. Chem. Phys.* **134**, 194502 (2011)
- ⁴⁵M. Tripathy and K. S. Schweizer, *J. Phys. Chem. B* **117**, 373 (2013)
- ⁴⁶N. E. Valadez-Pérez, A. L. Benavides, E. Schöll-Passinger, and R. Castañeda-Priego, *J. Chem. Phys.* **137**, 084905 (2012)
- ⁴⁷A. L. Benavides and F. Gámez, *J. Chem. Phys.* **135**, 134511 (2011)
- ⁴⁸A. L. Benavides, L. A. Cervantes, and J. Torres, *J. Phys. Chem. C* **111**, 16006 (2007)
- ⁴⁹J. R. Elliott and N. H. Gray, *J. Chem. Phys.* **123**, 184902 (2005)
- ⁵⁰J. Cui and J. R. Elliott, *J. Chem. Phys.* **116**, 8625 (2002)
- ⁵¹G. A. Chapela, L. E. Scriven, and H. T. David, *J. Chem. Phys.* **91**, 4307 (1989)
- ⁵²J. A. Barker and D. Henderson, *J. Chem. Phys.* **47**, 2856 (1967)
- ⁵³J. A. Barker and D. Henderson, *J. Chem. Phys.* **47**, 4714 (1967)
- ⁵⁴J. A. Barker and D. Henderson, *Phys. Rev. A* **1**, 1266 (1970)
- ⁵⁵A. Giacometti, C. Gögelein, F. Lado, F. Sciortino, S. Ferrari, and G. Pastore, *J. Chem. Phys.* **140**, 094104 (2014)
- ⁵⁶C. Gögelein, F. Romano, F. Sciortino, and A. Giacometti, *J. Chem. Phys.* **136**, 094512 (2012)
- ⁵⁷A. Kovalenko and F. Hirata, *J. Chem. Phys.* **110**, 10095 (1999)
- ⁵⁸A. Kovalenko and F. Hirata, *Chem. Phys. Lett.* **349**, 496 (2001)
- ⁵⁹D. J. Tildesley and W. B. Streett, *Mol. Phys.* **41**, 85 (1980)
- ⁶⁰M. S. Wertheim, *J. Chem. Phys.* **87**, 7323 (1987)
- ⁶¹D. Frenkel and B. Smit, *Understanding molecular simulations* (Academic, New York, 1996)
- ⁶²T. Morita and K. Hiroike, *Progr. Theor. Phys. (Japan)* **23**, 1003 (1960)
- ⁶³S. J. Singer and D. Chandler, *Mol. Phys.* **55**, 621 (1985)
- ⁶⁴L. W. Salvino and J. A. White, *J. Chem. Phys.* **96**, 4559 (1992)
- ⁶⁵D. Meeter and P. Wolfe, *Non-linear least squares* (University of Wisconsin Computing Center, 1965)
- ⁶⁶D. J. Kraft, J. Groenewold, and W. K. Kegel, *Soft Matter* **5**, 3823 (2009)